STUDIA UBB CHEMIA, LIX, 2, 2014 (p. 17-32)
(RECOMMENDED CITATION)

COMPUTATIONAL AND EXPERIMENTAL STUDY ON 7-EPICANDICANDIOL ISOLATED FROM *SIDERITIS NIVEOTOMENTOSA* HUBER – MORATHII

CEM BURAK YILDIZ[a,b], ZULEYHA OZER SAGIR[c], TURGUT KILIC[c,d] AND AKIN AZIZOGLU[a,*]

ABSTRACT. 7-epicandicandiol is an *ent*-kaurane diterpenoid isolated from *Sideritis niveotomentosa* Huber – Morathii. The molecular geometry, vibrational frequencies, and gauge including atomic orbital (GIAO) ^{1}H- and ^{13}C-NMR chemical shift values of the title compound in the ground state have been calculated using the Hartree–Fock and Density Functional Theory methods with the 6-31G(d) basis set, and compared with the experimental data. A detailed interpretations of the infrared and NMR spectra of 7-epicandicandiol are also reported. The results of the calculations were applied to unscaled theoretical wavenumbers of the title compound, which show good agreement with observed spectra.

Keywords: *terpenes, plants, IR spectrum, DFT, ab-initio*

INTRODUCTION

Terpenes are one of the main groups of secondary metabolites in nature showing a great diversity in structure and activity [1]. In industry, they are widely used as building blocks for pharmaceuticals, flavors, fragrances, food supplements and antioxidants [2]. Sideritis species are rich in diterpenes; at least 160 different diterpenes with a remarkable structural variability have been identified and isolated from the aerial parts [3]. 7-epicandicandiol, one of the *ent*-kaurane diterpenoids, can be isolated from the genus Sideritis (Lamiaceae). The Sideritis species are represented by

[a] *Department of Chemistry, Faculty of Arts and Sciences, Balikesir University, 10145, Balikesir, Turkey. Corresponding author: azizoglu@balikesir.edu.tr*
[b] *Department of Chemistry, Faculty of Arts and Sciences, Aksaray University, 68100, Aksaray, Turkey*
[c] *Altınoluk Vocational School, Balikesir University, Balikesir, Turkey*
[d] *Department of Science Education, Necatibey Faculty of Education,10145, Balikesir University, Balikesir, Turkey*

more than 150 species, which are distributed mainly in the Mediterranean and the Middle East [4]. 7-epicandicandiol has the antibacterial, antifeedant and toxicity activity [5-7]. Especially, it has been found that 7-epicandicandiol compound inhibits colon cancer moderately [8]. In addition to that, the compounds, 7-epicandicandiol and 7-epicandicandiol diacetate, which are isolated from *Sideritis trojana* have shown good insecticidal activity against to harmful insects [8].

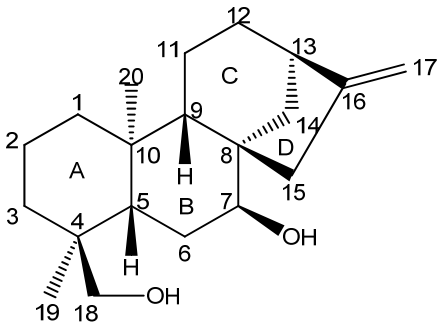

Figure 1. Structure of 7-epicandicandiol

The application of computational predictions, together with experimental methods, is currently limited in the natural products field. However, it has been growing rapidly in the last few years by the successful use of ^{1}H- and ^{13}C-NMR calculated chemical shifts and IR vibrations for structure identification, structure reassignment, and confirmation of natural products. The theoretical methods, such as the density functional theory (DFT), have become the dominant computational tools for dealing with organic molecules, isolated from plants [9-11]. Literature survey reveals that to the best of our knowledge no ab-initio (HF) and DFT calculations of 7-epicandicandiol have been reported so far. It may be due to difficulty in interpreting the results of calculations because of their complexity and low symmetry. Density functional theory (DFT) approaches using hybrid functional are frequently used to study the structural characteristics, vibrational and electronic properties, interactions among different orbitals. Hence, we wish to calculate geometrical parameters, fundamental frequencies and GIAO ^{1}H- and ^{13}C-NMR values of the title compound to distinguish the findings from the experimental ^{1}H- and ^{13}C-NMR values, vibrational frequencies, and geometric parameters, by using the HF and DFT methods with 6-31G(d) basis set. A comparison of the experimental and computational spectra can be very useful in making correct assignments and understanding the basic molecular structure [9-12].

RESULTS AND DISCUSSION

Molecular Structure

In this study, the geometry obtained from X-ray diffractometer was used as input for the full geometry optimization at the HF and DFT methods, together with the 6-31G(d) basis set. The general molecular structure and numbering of the atoms of 7-epicandicandiol is depicted in Figure 1. The optimized geometry calculated by the RB3LYP/6-31G(d) method is visualized in Figure 2.

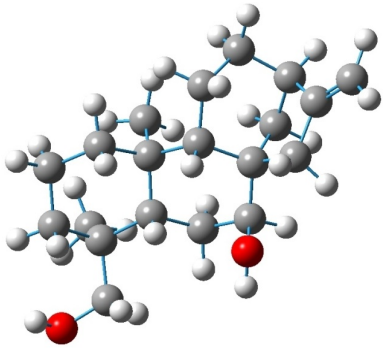

Figure 2. The optimized structure of 7-epicandicandiol achieved by RB3LYP/6-31G(d) method

The theoretically computed structural parameters can be compared with X-ray structure, which have been reported before [13]. The results of optimized parameters (bond lengths, bond angles, and dihedral angles) and experimentally predicted structural data of 7-epicandicandiol are listed in Table 1. As an example, the optimized bond lengths (C4-C5, C7-C8, C16-C17) of 7-epicandicandiol are determined to be 1.564, 1.529 and 1.318 Å for the RHF/6-31G(d) method and 1.568, 1.535 and 1.333 Å for the RB3LYP/6-31G(d) method, which are in much better agreement with that of experimental values 1.563, 1.527 and 1.350 Å, respectively. On the other hand, RHF/6-31G(d) method is insufficient at calculations of C-O bond lengths. For instance, the optimized C7-O7’ and C18-O18′ bond length by HF method are computed to be 1.414 and 1.405 Å, which are highly shorter than experimental data of 1.444 and 1.432 Å, respectively. Moreover, the theoretical

results of C-O bond lengths at RPW91/631G(d) method are much better agreement with experimentally predicted C-O bond lengths than the other theories. In general, all bond lengths and bond angles computed herein show good agreement with experimental findings. For instance, the correlation coefficient values (R^2) between experimental and theoretical bond lengths are found to be 0.9572, 0.9646, 0.965, 0.959, and 0.9517 for RHF, RPW91, RB3LYP, RPBE1PBE, and RLSDA, respectively.

Table 1. Optimized structural parameters (bond length (Å), bond angle (degree), and dihedral angle (degree)) of 7-epicandicandiol

Bond lengths	**Exp.**	RHF/ 6-31G(d)	RPW91/ 6-31G(d)	RB3LYP/ 6-31G(d)	RPBE1PBE/ 6-31G(d)	RLSDA/ 6-31G(d)
C1-C2	1.526	1.529	1.535	1.534	1.526	1.514
C1-C10	1.547	1.549	1.555	1.555	1.545	1.531
C2-C3	1.521	1.526	1.531	1.531	1.522	1.512
C3-C4	1.544	1.544	1.551	1.551	1.540	1.527
C4-C5	1.563	1.564	1.565	1.568	1.554	1.534
C4-C19	1.539	1.539	1.542	1.542	1.532	1.518
C4-C18	1.538	1.549	1.559	1.558	1.548	1.534
C5-C10	1.561	1.565	1.570	1.571	1.559	1.543
C7-C8	1.527	1.529	1.535	1.535	1.526	1.512
C7-O7’	1.444	1.414	1.441	1.436	1.423	1.414
C8-C14	1.542	1.546	1.554	1.553	1.543	1.531
C8-C15	1.548	1.555	1.563	1.563	1.551	1.538
C9-C10	1.567	1.578	1.583	1.584	1.571	1.553
C10-C20	1.543	1.543	1.545	1.546	1.536	1.523
C13-C16	1.510	1.516	1.521	1.520	1.513	1.504
C15-C16	1.476	1.520	1.523	1.523	1.515	1.503
C16-C17	1.350	1.318	1.341	1.333	1.331	1.332
C18-O18’	1.432	1.405	1.427	1.424	1.412	1.401
Bond angles						
C5-C4-C19	114	115	115	115	115	115
C4-C18-H18’	108	109	109	108	109	110
C7-O7’-(H-O7’)	105	109	106	107	107	107
C16-C17-H17’a	119	121	121	121	121	121
C16-C17-H17’b	120	121	121	121	121	121
C15-C16-C17	127	126	126	126	126	126
C13-C16-C17	125	126	125	126	126	125
H7’-C7-O7’	108	108	109	108	109	109
C9-C10-C20	112	112	112	112	112	112
C8-C7-O7’	109	107	107	107	107	106
O18’-C18-H18’a	108	104	104	104	104	105
O18’-C18-H18’b	108	110	110	110	110	111

Dihedral angles						
C4-C18-O18'-(H-O18')	-82	-72	-65	-62	-66	-61
(H-O18')-O18'-C18-H18'a	155	166	173	171	172	177
(H-O18')-O18'-C18-H18'b	39	51	58	56	56	61
H7'- C7-O7'-(H-O7')	-41	-57	-65	-62	-64	-71
C15-C16-C17-H17'a	179	178	178	178	178	178
C16-C15-C8-C14	30	30	30	30	30	31
C18-C4-C5-C6	61	60	61	61	61	61
C19-C4-C18-O18'	-60	-65	-63	-63	-64	-63

Vibrational Analysis

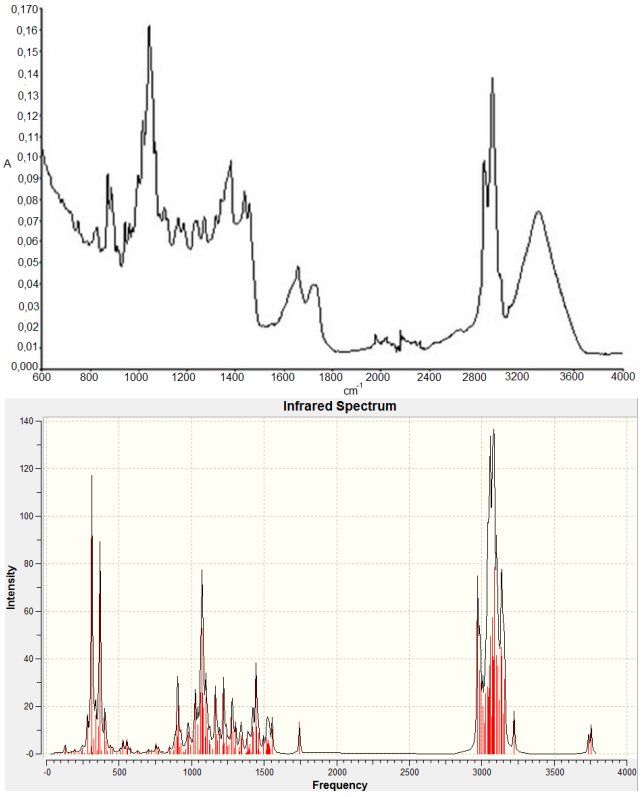

Figure 3. Visualization of experimental (above) and theoretical (below at RB3LYP/6-31G(d) level) IR spectra of 7-epicandicandiol

The title molecule has 54 atoms which have 156 normal modes from 57 to 4127 cm^{-1} at the RHF/6-31G(d) level, 56 to 3755 cm^{-1} at RB3LYP/6-31G(d) level, 57 to 3818 cm^{-1} at the RPBE1PBE/6-31G(d) level, 56 to 3637 cm^{-1} at the RPW91/6-31G(d) level, and 57 to 3647 cm^{-1} at the RLSDA/6-31G(d) level. It agrees with C1 point group symmetry, all vibrations are active in infrared absorption. In order to facilitate assignment of the observed peaks, we have analyzed vibrational frequencies and compared our calculation with experimental measurements (Table 2). On an absolute scale, it is well known that experimental results of infrared spectroscopy are usually lower than the corresponding computational quantities due to the combination of electron correlation effects and basis set deficiencies [10]. The experimental and theoretical FT-IR spectra are presented in Figure 3. The correlation coefficient (R^2) values between experimental and theoretical FT-IR results are calculated to be 0.9838, 0.9905, 0.9906, 0.9882, and 0.9884 for theories of RHF, RPW91, RB3LYP, RPBE1PBE, and RLSDA, respectively. In total, the RB3LYP/6-31G(d) has higher R^2 (0.9906) value than others. Hence, we have chosen the RB3LYP method as reference theoretical IR spectra for Figure 3. The IR spectra of the title structure are dominated by a broad and intense absorption in the range between 1000-3300 cm^{-1} for O-C and O-H vibrations.

The O–H group vibrations show pronounced shifts in the spectra of the hydrogen-bonded species, so they are most sensitive [14]. The absorption of free O-H group is existed in the region 3700-3580 cm^{-1}, whereas the intermolecular hydrogen bond formation can reduce the O-H stretching frequency to the 3550-3200 cm^{-1} region with increase in intensity [15]. The compound has two O-H groups. For the title compound, the both O-H groups give rise to broad band at about 3303 cm^{-1} for the vibration namely stretching. The stretching vibration have been calculated in the range from 3623.0 to 4127.0 cm^{-1} at the RHF/6-31G(d), RPW91/6-31G(d), RB3LYP/6-31G(d), RPBE1PBE/6-31G(d), and RLSDA/6-31G(d) theory of levels (Table 2). The calculated rocking vibrations of O-H groups are also observed in the range of 272-442 cm^{-1}. The theoretical results depict that the RPW91/6-31G(d) method shows better agreement with the experimental value of 3303.0 cm^{-1} than others for describing of O-H group vibration.

The C-O stretching mode is normally assigned near 1200 cm^{-1} for siderol and its derivatives [10,16]. The molecule has two C-O symmetrical stretching vibrations. In the present study, the stretching vibrations of the C–O are appeared at 1018 cm^{-1} (C18) and 1043 cm^{-1} (C7) in the FT-IR

spectrum. The theoretically predicted wavenumbers were found at 1181 cm^{-1} (C18) and 1205 cm^{-1} (C7) in the RHF/6-31G(d), 1044,1070 cm^{-1} (C18) and 1050 cm^{-1} (C7) in the RPW91/6-31G(d), 1082 cm^{-1} (C18) and 1099 cm^{-1} (C7) in the RB3LYP/6-31G(d), 1107, 1111 cm^{-1} (C18) and 1122 cm^{-1} (C7) in the RPBE1PBE/6-31G(d), 1091 cm^{-1} (C18) and 1099 cm^{-1} (C7) in the RLSDA/6-31G(d). The C-O symmetrical stretching frequencies obtained through the RPW91/6-31G(d) methodology are in excellent agreement with the experimental values reported above.

The ring stretching vibrations are very important due to characteristic nature in the IR spectrum. The C–C stretching vibrations of the ring appear in the range of 1625–1400 cm^{-1} [17]. In this study, experimental C-C bands observed at 1437.0 and 1458.0 cm^{-1}, which are in good agreement with calculated result of 1461.0 cm^{-1} at the RHF/6-31G(d) theory of level. The RHF/6-31G(d), RPW91/6-31G(d), RB3LYP/6-31G(d), RPBE1PBE/6-31G(d), and RLSDA/6-31G(d) theory of levels were performed to analyze the C=C peak absorption, which are 1893.0, 1695.0, 1744.0, and 1767.0, and 1732.0 cm^{-1}, respectively. The RPW91/6-31G(d) level shows better agreement with experimental observation (1660.0 cm^{-1}) than other methods for determination of the C=C signal.

Table 2. Assignment of the observed and calculated FT-IR spectra using RHF/6-31G(d), RPW91/6-31G(d), RB3LYP/6-31G(d), RPBE1PBE/6-31G(d), and RLSDA/6-31G(d) theory of levels for 7-epicandicandiol

Exp. (cm^{-1})	RHF/ 6-31G(d)	RPW91/ 6-31G(d)	RB3LYP/ 6-31G(d)	RPBE1PBE/ 6-31G(d)	RLSDA/ 6-31G(d)	*Approximate description*
	139	128	129	132	132	H-O-CH_2 rocking (C18)
	279, 296, 318	273, 301	282, 312	281, 311	272, 299	O-H rocking (C7)
	348, 359, 374, 376, 385	371	338, 369, 402	442, 376, 403	381, 403	O-H rocking (C18)
	406, 546, 596	492, 537	508, 552	509, 555	495	C=C-CH_2 rocking
873	753, 785, 909	702, 689	705, 724	694, 714, 729	702, 710	C=CH_2 twisting (C18)
	991	896	919	914, 930	904	H-O-CH_2 rocking
944	1023, 1024, 1046	859	900, 903, 906	899, 906	848, 854, 863	C=CH_2 wagging
1018	1181	1044,1070	1082	1107, 1111	1091	O-C symmetrical stretching C18)
1043	1205	1050	1099	1122	1099	O-C symmetrical stretching (C7)
	1256	1240	1278	1284	1237	H-O-CH_2 twisting (C18)
	1419	1250	1294	1293	1330	C=C-CH_2 wagging

Exp. (cm^{-1})	RHF/ 6-31G(d)	RPW91/ 6-31G(d)	RB3LYP/ 6-31G(d)	RPBE1PBE/ 6-31G(d)	RLSDA/ 6-31G(d)	*Approximate description*
	1581, 1587, 1667	1406,1400	1450, 1403	1447, 1403	1338,1374	H-O-CH_2 wagging (C18)
	1591	1429	1473	1468, 1470	1401,1404	C=CH_2 scissoring
	1624	1443	1495	1486	1416	C=C-CH_2 scissoring
	1573	1488	1522,1528, 1532, 1538	1525, 1521, 1533	1456	H-O-CH_2 scissoring (C18)
	1165, 1230	1094,1129	1172, 1220	1142, 1155, 1228	1104	C=C-CH_2 twisting
1660	1893	1685	1744	1767	1732	C=C symmetrical stretching
2854	3169	2888	2972	3000	2866	H-O-CH symmetrical stretching (C7)
2924	3180	2900	2983	2991	2870	H-O-CH_2 symmetrical stretching (C18)
	3241	3013	3072	3104	3015	H_2C=C-CH symmetrical stretching
	3222	2980	3048	3069	3087	C=C-CH_2 symmetrical stretching
	3276	3036	3222	3128	3170	C=C-CH_2 asymmetrical stretching
	3301	3036	3111	3132	3018	H-O-CH_2 asymmetrical stretching (C18)
3000	3316	3079	3149	3175	3087	C=CH_2 symmetrical stretching
	3388	3166	3222	3255	3170	C=CH_2 asymmetrical stretching
3303	4103	3653	3736	3802	3647	O-H symmetrical stretching (C7)
3303	4127	3637	3755	3818	3645	O-H symmetrical stretching (C18)

The vibrations show presence of C-H stretching in the region 3000–3100 cm^{-1}. In this molecule, the symmetrical stretching vibrations of C-H are observed at 2854, 2924 and 3000 cm^{-1} as medium strong band in the IR spectrum of title molecule. The computed wavenumbers for the same mode are assigned in the range of 2972–3149 cm^{-1}. In general, the experimental values agree well with the computed values from all theories used herein.

NMR spectra

The GIAO/DFT (Gauge including atomic orbital/density functional theory) approach is widely used for the NMR calculations [18]. In general, the proton chemical shift of the molecules varies greatly with the electronic environment of the proton. Hydrogen atoms, which are attached the electron-withdrawing atom or group, can decrease the shielding. In this case, the resonance of attached proton is altered towards to a higher frequency, whereas electron-donating atom or group increases the shielding and

moves the resonance towards to a lower frequency [19]. In the present investigation, the calculations of the chemical shift values for carbon atoms were performed by adopting the procedure recommended by Cheeseman et al. [20]. After that, GIAO ^{1}H- and ^{13}C-NMR chemical shift values (with respect to TMS) have been calculated using DFT and HF methods with 6-31G(d) basis set. The findings from theoretical methods were compared to the experimental ^{1}H-NMR and ^{13}C-NMR chemical shift values reported in ppm relative to TMS. The experimental and computed NMR results are tabulated in Table 3 and 4.

Table 3. Experimental and calculated ^{13}C-NMR chemical shifts (GIAO method) of 7-epicandicandiol

Carbon No	Exp. (ppm)	RB3LYP/ 6-31G(d)	RPBE1PBE/ 6-31G(d)	RSVWN/ 6-31G(d)	RPW91PW91/ 6-31G(d)	RHF/ 6-31G(d)
C1	39	33	27	35	35	32
C2	17	13	7	11	14	15
C3	38	27	22	29	30	28
C4	37	31	23	26	33	29
C5	38	37	30	37	39	34
C6	28	24	18	25	26	25
C7	77	69	62	70	73	65
C8	50	42	33	39	44	37
C9	50	45	37	45	47	41
C10	39	34	25	29	36	30
C11	17	13	7	11	15	14
C12	34	28	22	30	31	27
C13	43	38	32	38	41	35
C14	35	33	27	35	35	31
C15	45	38	33	41	41	38
C16	154	140	136	142	141	147
C17	103	93	91	95	94	101
C18	70	67	61	70	70	64
C19	18	9	5	10	11	14
C20	17	11	7	14	13	15

Table 4. Experimental and calculated ^{1}H-NMR chemical shifts (GIAO method) of 7-epicandicandiol

Proton No	Exp. (ppm)	RB3LYP/ 6-31G(d)	RPBE1PBE/ 6-31G(d)	RSVWN1/ 6-31G(d)	RPW91PW91/ 6-31G/(d)	RHF/ 6-31G(d)
H(1'a)	-	1,51	1,62	2,66	2,00	1,20
H(1'b)	-	0,64	0,69	1,53	1,07	0,39
H(2'a)	-	1,47	1,54	2,57	1,95	1,11
H(2'b)	-	1,13	1,23	2,11	1,56	0,98
H(3'a)	-	0,61	0,64	1,41	1,02	0,38
H(3'b)	-	1,25	1,31	2,14	1,67	1,04
H(5')	-	1,59	1,66	2,81	2,23	0,90
H(6'a)	-	1,53	1,60	2,75	2,10	0,98
H(6'b)	-	0,73	0,82	1,79	1,22	0,44
H(7')	3,66	3,38	3,35	4,38	3,88	2,80
H(9')	-	1,50	1,53	2,60	2,05	0,92
H(11'a)	-	1,22	1,30	2,29	1,70	0,89
H(11'b)	-	1,38	1,47	2,56	1,88	0,99
H(12'a)	-	1,23	1,30	2,17	1,67	1,00
H(12'b)	-	1,42	1,52	2,60	1,94	1,05
H(13')	2,69	2,25	2,32	3,23	2,73	2,03
H(14'a)	-	1,56	1,68	2,78	2,10	1,12
H(14'b)	-	0,95	1,03	1,97	1,44	0,61
H(15'a)	-	2,24	2,32	3,26	2,70	1,95
H(15'b)	-	2,23	2,29	3,15	2,68	1,92
H(17'a)	4,80	4,51	4,73	5,43	4,33	4,61
H(17'b)	4,80	4,58	4,79	5,45	4,95	4,70
H(18'a)	3,47	3,14	2,74	4,11	3,56	2,98
H(18'b)	2,92	2,74	3,22	3,54	3,18	2,44
H(19'a)	0,69	0,41	0,49	1,29	0,80	0,34
H(19'b)	0,69	0,68	0,76	1,53	1,06	0,59
H(19'c)	0,69	1,11	1,19	2,06	1,50	1,04
H(20'a)	1,05	0,89	0,99	1,94	1,36	0,64
H(20'b)	1,05	0,99	1,09	2,10	1,47	0,69
H(20'c)	1,05	0,56	0,68	1,66	1,00	0,38

As can be seen from Table 3 and 4, the calculated chemical shifts are mostly in agreement with the experimental findings. Comparing theoretical and experimental data, the correlation values of carbon and proton shifts are found to be 0.9909 and 0.9604 for the RHF/6-31G(d), 0.9941 and 0.9798 for the B3LYP/6-31G(d), 0,9944 and 0,9592 for the RPE1PBE/6-31G(d), 0,9889 and 0,9809 for the RSVWN1/6-31G(d), 0,9918 and 0,971 for the RPW91PW91/6-31G(d). However, the predicted chemical shifts from

PBE1PBE theory of level are much lower than experimental values. It seems that we could not obtain correct ^{13}C-NMR values with the PBE1PBE theory of level. The calculated difference is in the range from 8 to 18 ppm. For instance, experimental ^{13}C-NMR chemical shift for C16 is determined to be 154 ppm, whereas that of theoretical value is 136 ppm at PBE1PBE theory of level. The computed difference is found to be very high with 18 ppm. The overall results display that PBE1PBE methodology in the ^{13}C-NMR calculations is not useful for this kind of organic molecules. On the other hand, the chemical shifts at HF and B3LYP methods are in good agreement with experimentally predicted ^{13}C-NMR shifts due to very close values (Table 3). The chemical shifts of C=C of organic molecules are usually observed in the range of 110-150 ppm. Moreover, the carbon atoms (C16 and C17) in the C=C bond are calculated in the range of 93-147 ppm, whereas the experimental ^{13}C-NMR values of C16 and C17 found to be 154 and 103 ppm, respectively. In this case, the HF method shows better agreement with 147 and 101 ppm for C16 and C17, respectively. As can be seen from Table 4, the experimental ^{1}H-NMR chemical shifts are also in good compliance with theoretical findings.

Frontier Molecular Orbitals

The frontier molecular orbitals, which are called HOMO (Highest Occupied Molecular Orbital) and LUMO (Lowest Unoccupied Molecular Orbital) are most important orbitals in molecular systems [21]. The HOMO–LUMO energy gap is an important kinetic stability index and it also reflects the chemical reactivity of a molecule [22-25]. A molecule with a small frontier orbital gap is more polarizable and is generally associated with a high chemical reactivity, low kinetic stability. In the case of 7-epicandicandiol, the calculated energy gap of ΔE= 0.257 eV is identified between the HOMO and LUMO with the help of RB3LYP/6-31G(d) level of theory (Figure 4). This small HOMO-LUMO energy gap explains that the title molecule has low chemical hardness and low excitation energies for corresponding excited states. The title molecule with small energy gap is also more polarizable than hard molecules. The HOMO and LUMO orbitals mainly populate on the C=C bond, which can describe most active sides of the title molecule.

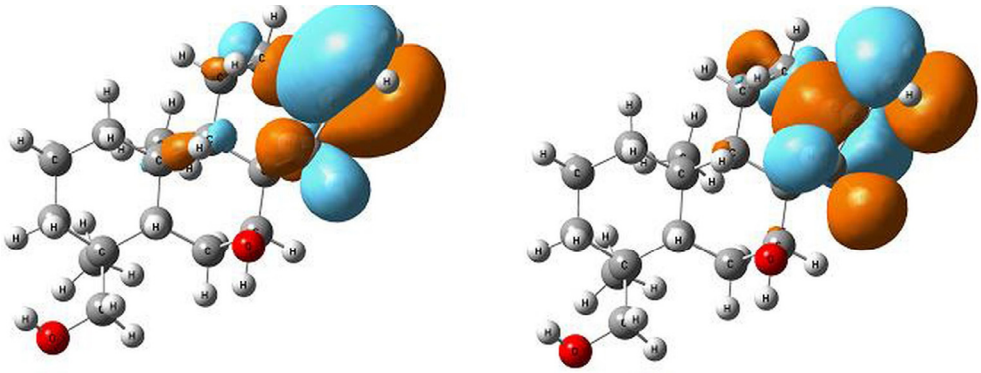

Figure 4. Molecular orbital surfaces and energies (in parentheses, eV) for the HOMO (left, -0.232 eV) and LUMO (right, 0.025 eV) of the 7-epicandicandiol computed at RB3LYP/6-31G(d) level

Molecular electrostatic potential (MEP) maps

The molecular electrostatic potential maps have used for interpreting and predicting for both electrophilic and nucleophilic behaviors in various chemical systems [26-28]. It also provides a visual method to understand the relative polarity of the molecule. In the MEPs, the most suitable atomic site for electrophilic attack is described as red color. On the other hand, the positive electrostatic potentials are appeared as blue surface areas. The MEP was calculated at the RB3LYP/6-31G(d) level for the title optimized geometry as shown in Figure 5. In view of this, we can say that the electron withdrawing hydroxyl substituents are increasing the chemical reactivity of a molecule. As can be seen from Figure 5, the oxygen atoms are covered by a greater surface of red color which describes most negative region of the molecule. The calculated value of mulliken charges on O7 and O18 are determined to be -0.636, and -0.623 at the RB3LYP/6-31G(d) theory of level, respectively. In addition to that, the terminal C atom of C=C bond has a relatively higher electronegative character (-0.440) than the other C atoms. Maximum positive regions are mainly over hydrogen atoms of OH groups with mulliken charges of 0.395 and 0.388. From this calculated results, we can conclude the behaviors of molecule in the electrophilic and nucleophilic reactions depending on its positive and negative sites.

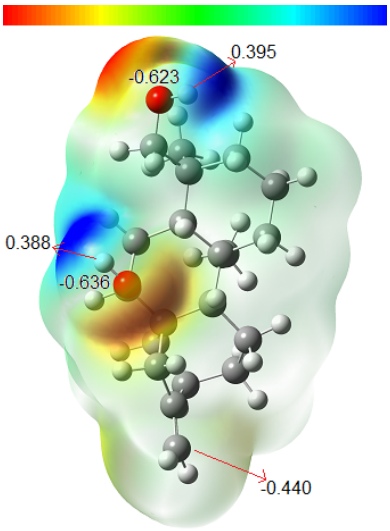

Figure 5. 3D-molecular electrostatic potential map of 7-epicandicandiol calculated at the RB3LYP/6-31G(d) level

CONCLUSIONS

In this study, we have calculated the geometric parameters (bond length, bond angle, dihedral angle), vibrational frequencies, infrared intensities, chemical shifts and thermodynamic parameters of 7-epicandicandiol by using HF and DFT methods with the 6-31G(d) basis set. The calculated vibrational frequencies have been compared with that of obtained experimental IR spectrum. Experimental fundamentals are found to have slightly a better correlation for B3LYP theory than other theories. Moreover, ^{1}H- and ^{13}C-NMR chemical shifts have been compared with experimental values. The computational results at the B3LYP/6-31G(d) method have shown better fit to experimental predictions than others in evaluating ^{1}H-NMR and ^{13}C-NMR chemical shifts. However, there is no sufficient agreement between experimental ^{13}C-NMR chemical shifts and the PBE1PBE method. The calculated structural parameters by B3LYP method closely matches with experimental X-Ray diffraction data. Especially, calculated bond lengths and angels at B3LYP and HF methods show much better agreement than other methods.

EXPERIMENTAL AND COMPUTATIONAL SECTION

The 7-epicandicandiol (ent-7-,18-dihydroxykaur-16-ene) having the ent-kaurene skeleton can be isolated from different species of Sideritis such as *Sideritis sipylea, S. trojana, S. niveotomentosa, S. chamaedrifolia, S. hirsuta, S. lurida, S. argyrea, S. condensata, S. congesta, S. huber-morathii, S. leptoclada, S. ozturkii* [29-32]. In our study, *Sideritis niveotomentosa Huber – Morathii* was collected from Sertuval highway between Mut and Karaman, Turkey at 1600 m altitude. The species were identified by Assoc. Prof. Dr. Tuncay Dirmenci from Balikesir Univ., Turkey. The isolation and experimental measurements on 7-epicandicandiol have been made according to previously reported procedure [10].

In the present work, the electronic structure calculations are performed using Gaussian 03 program suite [33]. The ground state of investigated system was performed using Hartree–Fock (HF) and Density functional theoretical (DFT) levels with using the 6-31G(d) basis set [34,35]. The restricted formalism was used for all calculations. In this study, the geometry was obtained from X-ray diffraction because of the large number of possible conformations for title compound. Firstly, equilibrium geometry was fully optimized without any constraints at RHF/6-31G(d) level. The results of HF/6-31G(d) calculations were repeated with full geometry optimization at higher DFT levels for better description. The optimized structural parameters were used in the vibrational frequency calculations at both HF and DFT levels to characterize all stationary points as minima. The geometry of the title compound, together with that of tetramethylsilane (TMS) is fully optimized. The ^{1}H- and ^{13}C-NMR values are calculated within GIAO approach applying the B3LYP and HF method with the 6-31G(d) basis set. Finally, the frontier molecular orbitals (FMOs) and molecular electrostatic potential map (MEP) were also calculated at the B3LYP/6-31G(d) level. The computed structures were visualized by using the GaussView 3.0 program [36].

ACKNOWLEDGMENTS

The authors wish to thank TUBITAK (Grant Number: TBAG-105T430) for generous financial supports.

REFERENCES

[1]. J. Gershenzon, N. Dudareva, *Nat. Chem. Bio.,* **2007**, *3*, 408.
[2]. I. Khalaf, L. Vlase, B. Ivanescu, D. Lazar, A. Corciova, *Studia UBB Chemia,* **2012**, *57*, 113.
[3]. E. González-Burgos, M.E. Carretero, M.P. Gómez-Serranillos, *J. Ethnopharmacol.* **2011**, *135,* 209.
[4]. E. Kupeli, F.P. Sahin, İ. Çalıs. E. Yeşilada, N. Ezer, *J. Ethnopharmacol.* **2007**, *112,* 356.
[5]. T. Kilic, *Molecules,* **2006**, *11*, 257.
[6]. G. Topcu, A.C. Gören, *Rec.Nat. Prod.*, **2007**, *1*, 1.
[7]. I. Aslan, T. Kilic¸ A.C. Gören, G. Topcu, *Indust. Crops and Prod.*, **2006**, *23*, 171.
[8]. T. Kilic, Y.K. Yıldız, A.C. Gören, G. Tümen, G. Topcu, *Chem. Nat. Comp.*, **2003**, *39,* 453.
[9]. D.S.O. Silva, M.J.C. Corrêa, H.R. Bitencourt, W.R. Monteiro, J. Lameira, L.S. Santos, G.M.S.P. Guilhon, D.S.B. Brasil, *J. Comput. Theor. Nanosci.*, **2012**, *9*, 953.
[10]. A. Azizoglu, Z. Özer, T. Kilic, *Collect. Czech. Chem. Commun.,* **2011**, *76*, 95.
[11]. S.D.O. Silva, R.N.S. Peixoto, J.R.A. Silva, C.N .Alves, *Int. J. Mol. Sci.,* **2011**, *12*, 9389.
[12]. A. Cansız, A. Cetin, C. Orek, M. Karatepe, K. Sarac, A. Kus, P. Kopari, *Spectrochim. Acta Part A*, **2012***, 97*, 606.
[13]. A. Linden, F. P. Şahin, N. Ezer, I. Çalış, *Acta Cryst. Section C*, **2006**, *62*, 253.
[14]. D. Bulgariu, R. Constantin, L. Bulgariu, *Studia UBB Chemia*, **2013**, *58*, 121.
[15]. G. Topçu, A.C. Gören, T. Kiliç, Y.K. Yildiz, G. Tümen, *Fitoterapia*, **2001**, *72*, 1.
[16]. S. Çarıkçı, C. Cöl, T. Kılıc, A. Azizoglu, *Rec. Nat. Prod.,* **2007**, *1*, 44.
[17]. D.RH. Olguin, M. Villa, M.L. Senent, M.A.M. Delgado, *J. Mex. Chem. Soc.*, **2008**, *52*, 98.
[18]. O.G. Beltran, J.S. Delgado, P.I. Vasquez, C. Areche, B.K. Cassels, *J. Chil. Chem. Soc.*, **2012**, *57*, 1323.
[19]. E. Kose, A. Atac, M. Karabacak, C. Karaca, M. Eskici, A. Karanfil, *Spectrochim. Acta Part A*, **2012**, *97*, 435.
[20]. J.R. Cheeseman, G.W. Trucks, T.A. Keith, M.J. Frisch, *J. Chem. Phys.*, **1996**, *104*, 5497.
[21]. I. Fleming, "Frontier Orbitals and Org. Chemical Reactions", Wile, London, **1976**.
[22]. B. Cicek, U. Cakir, A. Azizoglu, *J. Incl. Phenom. Macrocycl. Chem.,* **2012**, *72*, 121.
[23]. L. Găină, I. Torje, E. Gal, A. Lupan, C. Bischin, R. Silaghi-Dumitrescu, G. Damian, P. Lönnecke, C. Cristea, L. Silaghi-Dumitrescu, *Dyes Pigm.*, **2014**, *102*, 315.
[24]. V. Bucila, M. Stefu, B. Szefler, *Studia UBB Chemia*, **2013**, *58*, 101.

[25]. C.B. Yildiz, A. Azizoglu, *Struc. Chem.*, **2012**, *23*, 1777.
[26]. C.B. Yildiz, A. Azizoglu, *Comp. Theor. Chem.*, **2013**, *1023*, 24.
[27]. I. Sen, C.B. Yıldız, H. Kara, A. Azizoglu, *Phosphorus, Sulfur, and Silicon*, **2013**, *188*, 1621.
[28]. A. Azizoglu, C. B. Yıldız, *J. Organomet. Chem.*, **2012**, *715*, 19.
[29]. G. Topçu, A.C. Gören, T. Kılıç, Y.K. Yıldız, G. Tümen, *Turk. J. Chem.*, **2002**, *26*, 189.
[30]. G. Topçu, A.C. Gören, T. Kılıç, Y.K. Yıldız, G. Tümen, *Nat. Prod. Lett.*, **2002**, *16*, 33.
[31]. S. Çarıkçı, T. Kılıç, A. Azizoglu, G. Topçu, *Rec. Nat. Prod.*, **2012**, *6*, 101.
[32]. M.F. Braulio, *Phytochemistry*, **2012**, *76*, 7.
[33]. Gaussian 03, Revision C.02, M.J. Frisch, G.W. Trucks, H.B. Schlegel, G.E. Scuseria, M.A. Robb, J.R. Cheeseman, J.A. Montgomery, Jr., T. Vreven, K. N. Kudin, J.C. Burant, J.M. Millam, S.S. Iyengar, J. Tomasi, V. Barone, B. Mennucci, M. Cossi, G. Scalmani, N. Rega, G.A. Petersson, H. Nakatsuji, M. Hada, M. Ehara, K. Toyota, R. Fukuda, J. Hasegawa, M. Ishida, T. Nakajima, Y. Honda, O. Kitao, H. Nakai, M. Klene, X. Li, J.E. Knox, H.P. Hratchian, J.B. Cross, V. Bakken, C. Adamo, J. Jaramillo, R. Gomperts, R.E. Stratmann, O. Yazyev, A.J. Austin, R. Cammi, C. Pomelli, J.W. Ochterski, P. Y. Ayala, K. Morokuma, G.A. Voth, P. Salvador, J.J. Dannenberg, V.G. Zakrzewski, S. Dapprich, A.D. Daniels, M.C. Strain, O. Farkas, D.K. Malick, A.D. Rabuck, K. Raghavachari, J.B. Foresman, J.V. Ortiz, Q. Cui, A.G. Baboul, S. Clifford, J. Cioslowski, B.B. Stefanov, G. Liu, A. Liashenko, P. Piskorz, I. Komaromi, R.L. Martin, D.J. Fox, T. Keith, M.A. Al-Laham, C.Y. Peng, A. Nanayakkara, M. Challacombe, P.M.W. Gill, B. Johnson, W. Chen, M.W. Wong, C. Gonzalez, and J.A. Pople, Gaussian, Inc., Wallingford CT, **2004**.
[34]. W.J. Hehre, L. Radom, P.V.R. Schleyer, J. Pople, “Ab initio molecular orbital theory”, Wiley, New York, **1986**.
[35]. F. Jensen, “Introduction to computational chemistry”, Wiley, West Sussex, England, **1999**.
[36]. GaussView, Version 3.09, R. Dennington, T. Keith, J. Millam, K. Eppinnett, W.L. Hovell, R. Gilliland, Semichem, Inc., Shawnee Mission, KS, **2003**.